Current Medicinal Chemistry, 1999, *6*, 635-664

Pharmacology of Cannabinoid Receptor Ligands

Roger G. Pertwee

Department of Biomedical Sciences, Institute of Medical Sciences, University of Aberdeen, Foresterhill, Aberdeen AB25 2ZD, Scotland

Abstract: Mammalian tissues contain at least two types of cannabinoid receptor, CB_1 and CB_2, both coupled to G proteins. CB_1 receptors are expressed mainly by neurones of the central and peripheral nervous system whereas CB_2 receptors occur in certain non-neuronal tissues, particularly in immune cells. The existence of endogenous ligands for cannabinoid receptors has also been demonstrated. The discovery of this 'endogenous cannabinoid system' has been paralleled by a renewed interest in possible therapeutic applications of cannabinoids, for example in the management of pain and in the suppression of muscle spasticity/spasm associated with multiple sclerosis or spinal cord injury. It has also prompted the development of a range of novel cannabinoid receptor ligands, including several that show marked selectivity for CB_1 or CB_2 receptors. This review summarizes current knowledge about the in vitro pharmacological properties of important CB_1 and CB_2 receptor ligands. Particular attention is paid to the binding properties of these ligands, to the efficacies of cannabinoid receptor agonists, as determined using cyclic AMP or [^{35}S]GTPγS binding assays, and to selected examples of how these pharmacological properties can be influenced by chemical structure. The in vitro pharmacological properties of ligands that can potently and selectively oppose the actions of CB_1 or CB_2 receptor agonists are also described. When administered by themselves, some of these ligands produce effects in certain tissue preparations that are opposite in direction to those produced by cannabinoid receptor agonists and the possibility that the ligands producing such 'inverse cannabimimetic effects' are inverse agonists rather than pure antagonists is discussed.

Introduction

An important recent advance in the field of cannabinoid research has been the discovery of the presence in mammalian tissues of at least two types of cannabinoid receptor, CB_1 and CB_2 [1, 2]. Both receptor types have been cloned, their predicted amino acid sequences showing a similarity of about 44% (35% to 82% within the individual transmembrane domains) [3]. CB_1 and CB_2 receptors are coupled through G_i or G_o proteins, negatively to adenylate cyclase and to N- and P/Q-type calcium channels and positively to A-type and inwardly rectifying potassium channels and to mitogen activated protein kinase. Under certain conditions, CB_1 receptors may also act through G_s proteins to activate adenylate cyclase [4]. There is also evidence that CB_1 receptors may mobilize arachidonic acid and close 5-HT_3 receptor ion channels when activated [1]. In addition, cannabinoids can close sodium channels but whether this effect is receptor-mediated has yet to be established [1].

As to the distribution pattern of cannabinoid receptors, CB_1 receptors are found mainly on neurones in the brain, spinal cord and peripheral nervous system and an important function of these receptors seems to be modulation of the release of several different transmitters at particular central and peripheral loci [1, 2]. The distribution of CB_1 receptors within the CNS is consistent with the ability of psychotropic cannabinoids to impair cognition and memory and to alter the control of motor function and the perception of pain. Thus the cerebral cortex, hippocampus, caudate-putamen, substantia nigra pars reticulata, globus pallidus, entopeduncular nucleus, cerebellum, central grey substance and dorsal horn of the spinal cord all contain significant numbers of CB_1 receptors [1, 2]. Although it is known that CB_2 receptors are expressed mainly by immune cells [1, 2], little is yet known about their physiological role.

The cloning of the CB_1 receptor in 1990 was followed by the demonstration in 1992 that mammalian tissues produce agonists for these receptors [1, 2]. The most important of these 'endocannabinoids' are arachidonoylethanolamide (anandamide) and 2-arachidonoyl glycerol (Fig. 1). Both these compounds are thought to serve as neuromodulators or neurotransmitters, there being evidence that they are synthesized within neurones, that they can undergo

0929-8673/99 $19.00+.00

depolarization-dependent release from neurones and that once released they are rapidly removed from the extracellular space by tissue uptake and intracellular metabolism [5, 6]. Cannabinoid CB_1 and CB_2 receptors and endocannabinoids together constitute the 'endogenous cannabinoid system'.

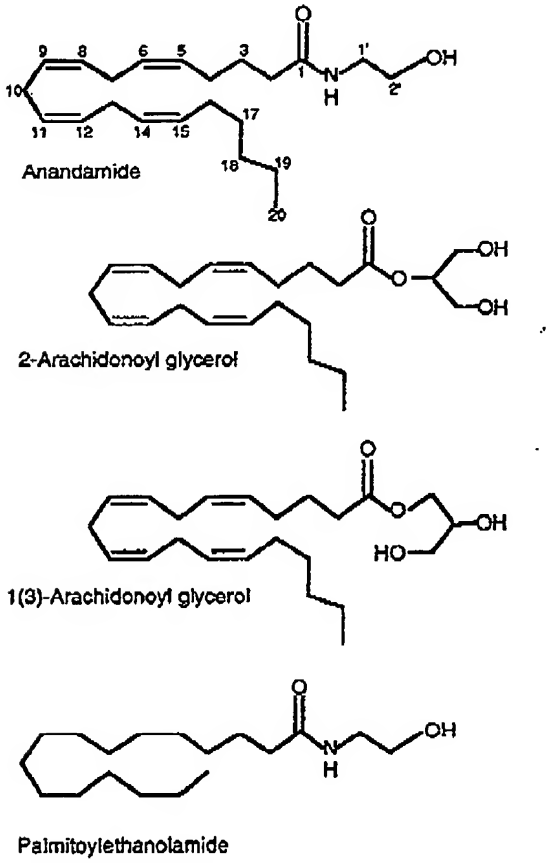

Fig. (1). Structures of anandamide, 1- and 2-arachidonoyl glycerol and palmitoylethanolamide.

The discovery of the endogenous cannabinoid system has prompted a search both for selective CB_1 and CB_2 receptor agonists and antagonists and for drugs that will selectively modulate the concentrations of endocannabinoids at their receptors, through effects on tissue uptake or enzymic hydrolysis. This review focuses on the pharmacological properties of just some of the many CB_1 and CB_2 receptor ligands that are now available. Included are Δ^9-tetrahydrocannabinol (Δ^9-THC), the main psychotropic constituent of cannabis, and nabilone (Fig. 2). Both these cannabinoids are licensed medicines [7]. Δ^9-THC, as the oral preparation dronabinol (Marinol), is available in the USA for the suppression of nausea and vomiting provoked by anticancer drugs and for the reversal, through appetite stimulation, of body weight loss experienced by AIDS patients. Nabilone (Cesamet), a synthetic analogue of Δ^9-THC that is also given by mouth, is licensed for use in the UK, again to suppress nausea and vomiting produced by cancer chemotherapy. Also included in this review is a range of compounds that are commonly used as experimental tools and/or that have therapeutic potential. Particular attention is paid to the affinities of these ligands for CB_1 and CB_2 receptors, to the extent that it has been possible to develop agents with selectivity for CB_1 or CB_2 receptors and to the relative efficacies of agonists at CB_1 and CB_2 receptors. The question of whether so called cannabinoid receptor antagonists are really inverse agonists is also addressed. Although no attempt has been made to give a complete account of what is now known about the structural features of compounds that determine cannabinoid receptor affinity or efficacy, mention is made of a few observations that have provided important insights into such structure-activity relationships. The review begins with a brief account of the various in vitro bioassay systems that are now most widely used to characterize cannabinoid receptor ligands.

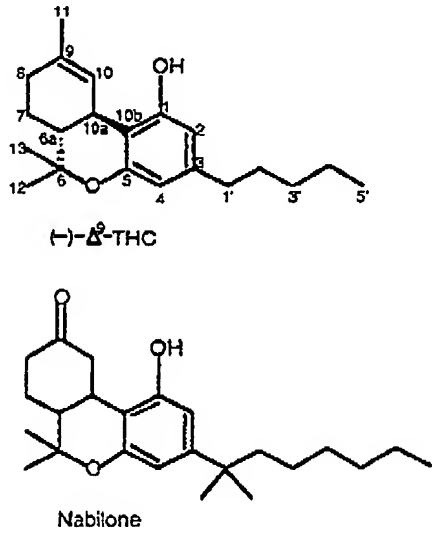

Fig. (2). Structures of (−)-Δ^9-tetrahydrocannabinol (Δ^9-THC) and nabilone.

Bioassay Systems for Determining the CB_1 and CB_2 Binding Properties and Pharmacological Activity of Cannabinoid Receptor Ligands

In vivo assays have played an important part in characterizing the pharmacology and structure activity relationships of ligands for CB_1 receptors [8] and remain important for determining the acute and chronic pharmacological and toxicological profiles of cannabinoids in the whole organism. However, for establishing the pharmacological properties of any novel cannabinoid, particularly its CB_1 and CB_2 receptor affinity and efficacy, the starting point now must be the

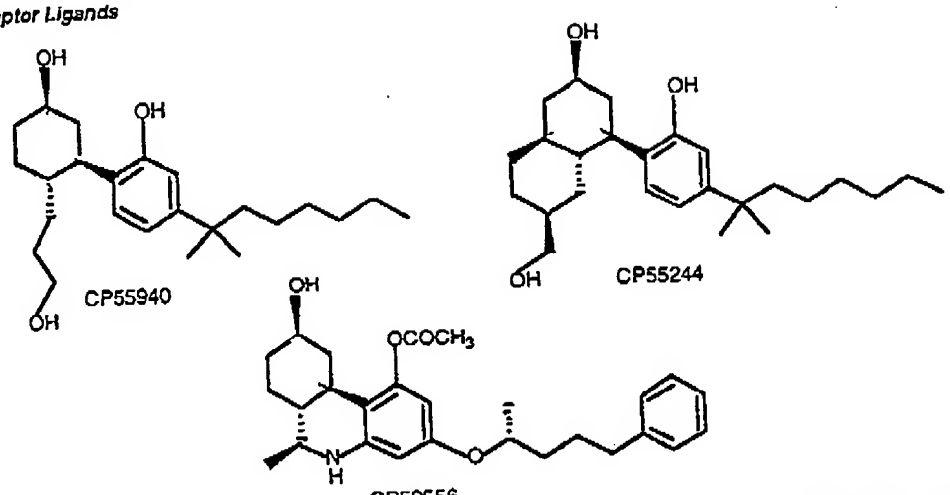

Fig. (3). Structures of CP55940, CP55244 and CP50556 (L-nantradol). The (+)-enantiomer of CP55940 is CP56667.

small set of in vitro 'gold standard' bioassays described below.

Binding Assays with Radiolabelled Cannabinoid Receptor Probes

Several cannabinoid receptor ligands have been radiolabelled with tritium and these have played a vital part both in determining the affinities of unlabelled cannabinoids for CB_1 and CB_2 receptors in displacement assays and in establishing the tissue distribution of cannabinoid receptors [1]. Commercially available radiolabelled cannabinoid receptor ligands are [^{3}H]SR141716A, which is CB1-selective, and [^{3}H]CP55940, [^{3}H](+)-WIN55212 and [^{3}H]HU-243, which bind more less equally well to CB_1 and CB_2 receptors (Table 1). The structures of CP55940, WIN55212, SR141716A and [^{3}H]HU-243 are shown in Figs. 3 to 6.

Table 1. Dissociation Constant (K_D) Values of Radiolabelled Ligands at Specific CB_1 and CB_2 Binding Sites in Brain or Transfected Cell Membranes

Radioligand	Source of membranes	K_D (nM)	Reference
[^{3}H]SR141716A	Guinea-pig forebrain	1.24	[26]
	Rat cerebellum (10 brain areas studied)	0.19	[22]
	Rat cerebellum	0.50	[19]
	Rat cerebellum	0.59	[17]
	Rat cerebellum	0.61	[20]
	Rat brain minus cerebellum	0.61	[15]
	Primary culture of rat cortical neurones	0.76	[18]
	Rat brain	1.20	[25]
[^{123}I]AM251	Rodent cerebellum (3 brain areas studied)	0.25	[21]
[^{3}H](+)-WIN55212	Guinea-pig forebrain	2.34	[26]
	Rat cerebellum	1.89	[10]
	Rat cerebellum (10 brain areas studied)	4.67	[22]
	Rat cerebellum	8.60	[23]
	Rat CB_1 AtT-20 cells	2.60	[13]
	Human CB_1 293 cells	11.9	[16]
	Human CB_1 CHO cells	16.2	[24]
	Human CB_2 COS cells	2.10	[12]
	Human CB_2 COS cells	3.70	[11]
	Human CB_2 CHO cells	3.80	[12]
[^{3}H]HU-243	Rat brain minus brain stem	0.045	[9]
	Human CB_2 CHO cells	0.061	[14]
[^{3}H]CP55940	Human CB_1 cells	0.4 to 3.3	[1]
	Rat CB_1 cells	4.00	[1]
	Rat brain	0.07 to 2.3	[1]
	Mouse brain	3.4	[1]
	Human CB_2 cells	0.2 to 7.37	[1]
	Mouse CB_2 cells	0.394	[1]

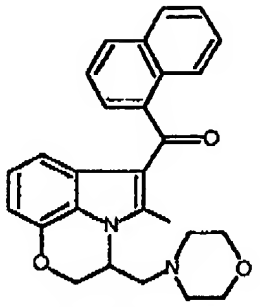

WIN55212

Fig. (4). Structure of WIN55212.

The most widely used radiolabelled cannabinoid is [^{3}H]CP55940. As this has the same affinity for CB_1 and CB_2 receptors, results obtained from displacement assays using this radioligand will only yield useful information about the binding properties of unlabelled compounds if they are performed with membranes that are known to contain either CB_1 or CB_2 receptors but not both. Ideally, these membranes should be obtained from CB_1 or CB_2 transfected cells. An alternative is to use tissue that expresses CB_1 or CB_2 receptors naturally, for example brain tissue for CB_1 receptors and spleen tissue for CB_2 receptors. Although often used, these tissues are less satisfactory for displacement binding assays than transfected cells. Thus although brain tissue is largely populated with CB_1 receptors, some CB_2 receptors may also be present, on neurones and astrocytes [27, 28]. Similarly, although most cannabinoid receptors in the spleen are CB_2, some CB_1 receptors are also present in this tissue [1]. There is also the possibility that brain and/or spleen express types of cannabinoid receptor yet to be identified. Indeed, there is already some evidence, albeit still inconclusive, that mammalian brain, spinal cord and peripheral nervous system can express additional cannabinoid receptor types/subtypes [28, 29]. Binding assays performed with membranes from brain, spleen or other cannabinoid-receptor containing tissues using well-characterized cannabinoid receptor ligands provide a powerful means of searching for novel cannabinoid receptor types/subtypes. Another commercially available radiolabelled cannabinoid receptor probe is [^{3}H]anandamide. However, this tends to be used in experiments designed to explore the biochemistry and pharmacology of anandamide tissue uptake and metabolism rather than in receptor binding assays. The CB_2-selective ligand, [^{3}H]SR144528 has also been synthesized but is not yet generally available. Representative CB_1/CB_2 K_D values of [^{3}H]SR141716A, [^{3}H]CP55940, [^{3}H](+)-WIN55212 and [^{3}H]HU-243 are shown in Table 1 whilst values for the relative CB_1/CB_2 affinities of unlabelled SR141716A, CP55940, (+)-WIN55212 and anandamide are given in Table 2.

Table 2. The Abilities of Certain Ligands to Bind to CB_1 and CB_2 Receptors

Displacing Ligand	Radioligand	CB_1 membranes	CB_2 membranes	CB_1 K_i (nM)	CB_2 K_i (nM)	Affinity ratio CB_1/CB_2	Affinity ratio CB_2/CB_1	Reference
CB_1 selective								
ACEA (Fig. 11)	[^{3}H]CP55940	Rat cerebellum	Rat spleen	1.4*	>2000*	>1428	<0.0007	[46]
SR141716A (Fig. 5)	[^{3}H]CP55940	hCB_1 in L cells	hCB_2 in CHO cells	11.8	13200	1118.64	0.00089	[42]
SR141716A	[^{3}H]CP55940	hCB_1 in L cells	hCB_2 in AtT-20 cells	11.8	973	82.46	0.012	[32]
SR141716A	[^{3}H]CP55940	hCB_1 in CHO cells	hCB_2 in CHO cells	12.3	702	57.07	0.018	[37]
SR141716A	[^{3}H]CP55940	hCB_1 in CHO cells	hCB_2 in CHO cells	5.6	>1000	>178.57	<0.0056	[30]
SR141716A	[^{3}H]CP55940	Rat brain†	Rat spleen	1.98	>1000	>505.05	<0.002	[30]
ACPA (Fig. 11)	[^{3}H]CP55940	Rat cerebellum	Rat spleen	2.2*	715*	325.00	0.0031	[46]
LY320135 (Fig. 14)	[^{3}H]CP55940	hCB_1 in L cells	hCB_2 in CHO cells	141	14900	105.67	0.0095	[42]
Methanandamide (Fig. 11)	[^{3}H]CP55940	Rat forebrain	Mouse spleen	17.9*	868*	48.49	0.021	[45]
Methanandamide	[^{3}H]CP55940	Rat forebrain	Mouse spleen	20*	815	40.75	0.025	[40]
O-585 (Fig. 11)	[^{3}H]CP55940	hCB_1 in CHO cells	hCB_2 in CHO cells	8.6*	324*	37.67	0.027	[37]
O-689 (Fig. 11)	[^{3}H]CP55940	hCB_1 in CHO cells	hCB_2 in CHO cells	5.7*	132*	23.16	0.043	[37]
Similar affinities for CB_1 and CB_2 receptors								
Anandamide (Fig. 1)	[^{3}H]CP55940	Rat forebrain	Mouse spleen	61*	1930*	31.64	0.032	[45]

(Table 2). contd....

Displacing Ligand	Radioligand	CB_1 membranes	CB_2 membranes	CB_1 K_i (nM)	CB_2 K_i (nM)	Affinity ratio CB_1/CB_2	Affinity ratio CB_2/CB_1	Reference
Anandamide	[^{3}H]CP55940	hCB_1 in CHO cells	hCB_2 in CHO cells	89*	371*	4.17	0.24	[37]
Anandamide	[^{3}H]CP55940	hCB_1 in L cells	hCB_2 in AtT-20 cells	543	1940	3.57	0.28	[32]
Anandamide	[^{3}H]CP55940	Rat cerebellum	Rat spleen	71.7*	279*	3.89	0.26	[46]
Anandamide	[^{3}H]CP55940	rCB_1 in COS cells	hCB_2 in COS cells	252	581	2.31	0.43	[31]
Anandamide	[^{3}H]HU-243	Rat forebrain	Mouse spleen	1760*	13000	7.39	0.14	[40]
AM404 (Fig. 12)	[^{3}H]CP55940	rCB_1 in COS cells	hCB_2 in CHO cells	32.3	170.5	5.28	0.19	[41]
CT-3 (Fig. 7)	[^{3}H]HU-243	rCB_1 in COS cells	hCB_2 in COS cells	472	1400	2.97	0.34	[31]
2-AG (Fig. 1)	[^{3}H]HU-243	CB_1 in COS cells	CB_2 in COS cells	58.3	145	2.49	0.40	[44]
2-AG	[^{3}H]HU-243	rCB_1 in COS cells	hCB_2 in CHO cells	0.1	0.2	2.00	0.50	[41]
11-OH-CBN-DMH (Fig. 8)	[^{3}H]HU-243	hCB_1 in L cells	hCB_2 in AtT-20 cells	0.0608	0.524	8.62	0.12	[32]
HU-210 (Fig. 6)	[^{3}H]CP55940	rCB_1 in COS cells	hCB_2 in CHO cells	0.1	0.17	1.70	0.59	[41]
HU-210	[^{3}H]HU-243	hCB_1 in CHO cells	hCB_2 in CHO cells	0.73	0.22	0.30	3.32	[37]
HU-210	[^{3}H]CP55940	hCB_1 in CHO cells	hCB_2 in CHO cells	1990	>10,000	>5.0	<0.2	[37]
HU-211 (Fig. 5)	[^{3}H]CP55940	hCB_1 in CHO cells	hCB_2 in CHO cells	5.25	7.41	1.41	0.71	[49]
O-1184 (Fig. 9)	[^{3}H]CP55940	hCB_1 in CHO cells	hCB_2 in CHO cells	53.3	75.3	1.41	0.71	[32]
Δ^9-THC (Fig. 2)	[^{3}H]CP55940	hCB_1 in L cells	hCB_2 in AtT-20 cells	39.5	40	1.01	0.99	[34]
Δ^9-THC	[^{3}H]HU-243	rCB_1 in COS cells	hCB_2 in COS cells	40.7	36.4	0.89	1.12	[37]
Δ^9-THC	[^{3}H]CP55940	hCB_1 in CHO cells	hCB_2 in CHO cells	80.3	32.2	0.40	2.49	[41]
Δ^9-THC	[^{3}H]HU-243	rCB_1 in COS cells	hCB_2 in CHO cells	35.3	3.9	0.11	9.05	[30]
Δ^9-THC	[^{3}H]CP55940	Rat brain†	Rat spleen	1.84	2.19	1.19	0.84	[33]
Nabilone (Fig. 2)	[^{3}H]CP55940	hCB_1	hCB_2	47.6	39.3	0.83	1.21	[36]
Δ^8-THC (Fig. 7)	[^{3}H]CP55940	Rat forebrain	Mouse spleen	0.241	0.199	0.83	1.21	[41]
Δ^9-THC-DMH (Fig. 7)	[^{3}H]HU-243	rCB_1 in COS cells	hCB_2 in CHO cells	2	1.5	0.75	1.33	[41]
CBN-DMH (Fig. 8)	[^{3}H]HU-243	rCB_1 in COS cells	hCB_2 in CHO cells	5	1.8	0.36	2.78	[47]
CP55940 (Fig. 3)	[^{3}H]CP55940	hCB_1 *in CHO cells*	hCB_2 in CHO cells	3.72	2.55	0.69	1.46	[32]
CP55940	[^{3}H]CP55940	hCB_1 in L cells	hCB_2 in AtT-20 cells	1.37	1.37	1.0	1.0	[30]
CP55940	[^{3}H]CP55940	Rat brain†	Rat spleen	0.58	0.69	1.19	0.84	[37]
CP55940	[^{3}H]CP55940	hCB_1 in CHO cells	hCB_2 in CHO cells	0.50*	2.80*	5.60	0.18	[46]
CP55940	[^{3}H]CP55940	Rat cerebellum	Rat spleen	38	26.6	0.70	1.43	[41]
11-OH-CBN (Fig. 8)	[^{3}H]HU-243	rCB_1 in COS cells	hCB_2 in CHO cells	4350	2860	0.66	1.52	[37]
Cannabidiol (Fig. 8)	[^{3}H]CP55940	hCB_1 in CHO cells	hCB_2 in CHO cells	211.2	126.4	0.60	1.67	[41]
Cannabinol (Fig. 8)	[^{3}H]HU-243	rCB_1 in COS cells	hCB_2 in CHO cells	308	96.3	0.31	3.20	[37]
Cannabinol	[^{3}H]CP55940	hCB_1 in CHO cells	hCB_2 in CHO cells	1130	301	0.27	3.75	[32]
Cannabinol	[^{3}H]CP55940	hCB_1 in L cells	hCB_2 in AtT-20 cells	61.7	23.6	0.38	2.61	[37]
CP56667 (Fig. 3)	[^{3}H]CP55940	hCB_1 in CHO cells	hCB_2 in CHO cells	25.8	7.4	0.29	3.49	[41]
11-OH-Δ^8-THC (Fig. 7)	[^{3}H]HU-243	rCB_1 in COS cells	hCB_2 in CHO cells	23	2.9	0.13	7.93	[38]
1-deoxy-Δ^8-THC-DMH (Fig. 10)	[^{3}H]CP55940	Rat cerebral cortex	hCB_2 in CHO cells					

(Table 2). contd....

Displacing Ligand	Radioligand	CB_1 membranes	CB_2 membranes	CB_1 K_i (nM)	CB_2 K_i (nM)	Affinity ratio CB_1/CB_2	Affinity ratio CB_2/CB_1	Reference
CB_2 selective								
(+)-WIN55212 (Fig. 4)	[^{3}H]CP55940	Rat brain†	Rat spleen	9.94	16.2	1.63	0.61	[30]
(+)-WIN55212	[^{3}H]CP55940	Rat cerebellum	Rat spleen	4.4*	1.2*	0.27	3.67	[46]
(+)-WIN55212	[^{3}H]CP55940	hCB_1 in CHO cells	hCB_2 in CHO cells	1.89	0.28	0.15	6.75	[37]
(+)-WIN55212	[^{3}H]CP55940	hCB_1 in L cells	hCB_2 in AtT-20 cells	62.3	3.3	0.053	18.88	[32]
(+)-WIN55212	[^{3}H]CP55940	hCB_1 in COS cells	hCB_2 in COS cells	123	4.1	0.033	30.00	[35]
JWH-015 (Fig. 13)	[^{3}H]CP55940	hCB_1 in CHO cells	hCB_2 in CHO cells	383	13.8	0.036	27.75	[37]
JWH-051 (Fig. 10)	[^{3}H]CP55940	Rat cerebral cortex	hCB_2 in CHO cells	1.2	0.032	0.027	37.50	[38]
L768242 (Fig. 13)	[^{3}H]CP55940	hCB_1	hCB_2	1917	12	0.0063	159.75	[39]
JWH-139 (Fig. 10)	[^{3}H]CP55940	Rat cerebral cortex	hCB_2 in CHO cells	2290	14	0.0061	163.57	[48]
AM630 (Fig. 13)	[^{3}H]CP55940	hCB_1 in CHO cells	hCB_2 in CHO cells	5152	31.2	0.0061	165.13	[47]
JWH-133 Fig. 10)	[^{3}H]CP55940	Rat cerebral cortex	hCB_2 in CHO cells	677	3.4	0.005	199.12	[48]
1-deoxy-Δ^8-THC (Fig. 10)	[^{3}H]CP55940	Rat cerebral cortex	hCB_2 in CHO cells	8770	32	0.0037	274.1	[48]
L759633 (Fig. 10)	[^{3}H]CP55940	hCB_1 in CHO cells	hCB_2 in CHO cells	1043	6.4	0.0061	162.97	[47]
L759633	[^{3}H]CP55940	hCB_1	hCB_2	15850	20	0.0013	792.5	[33]
L759656 (Fig. 10)	[^{3}H]CP55940	hCB_1 in CHO cells	hCB_2 in CHO cells	4888	11.8	0.0024	414.24	[47]
L759656	[^{3}H]CP55940	hCB_1	hCB_2	>20000	19.4	<0.00097	>1000	[33]
SR144528 (Fig. 5)	[^{3}H]CP55940	hCB_1 in CHO cells	hCB_2 in CHO cells	437	0.60	0.0014	728.33	[43]
SR144528	[^{3}H]CP55940	Rat brain†	Rat spleen	305	0.30	0.00098	1016.67	[43]
SR144528	[^{3}H]CP55940	hCB_1 in CHO cells	hCB_2 in CHO cells	>10000	5.6	<0.00056	>1785	[47]

†Minus cerebellum. *With PMSF 50 to 300 μM.
CP56667 is the (+)-enantiomer of CP55940. HU-211 is the (+)-enantiomer of HU-210.
h, human; r, rat; ACEA, arachidonoyl-2-chloroethylamide; ACPA, arachidonoylcyclopropylamide; 2-AG, 2-arachidonoyl glycerol. CBN, cannabinol; DMH, dimethylheptyl; THC, tetrahydrocannabinol.

Three other radiolabelled ligands have been developed as potential probes for human single photon emission computed tomography (SPECT) or positron emission tomography (PET) studies, all analogues of SR141716A (Fig. 5). One of these is an [^{18}F]-labelled analogue, SR144385 [50]. Another is [^{123}I]AM251, in which the 4'-Cl of the monochlorophenyl group of SR141716A is replaced by 4'-I [21, 51] (Table 1). The third of these radiolabelled ligands is [^{123}I]AM281 in which the piperidine ring of SR141716A is replaced by a more polar morpholino group [52]. AM281antagonizes (+)-WIN55212-induced inhibition of evoked acetylcholine release in rat hippocampal slices with a similar potency to SR141716A [53]. Like SR141716A (see below), it also enhances evoked acetylcholine release in rat hippocampal slices when administered alone [53].

Functional In vitro Assays

Two in vitro bioassay systems have yielded most information about the efficacy of ligands at CB_1 and CB_2 receptors. One of these measures net agonist-stimulated [^{35}S]GTPγS binding to G protein (Table 3). It relies on one of the events triggered by the occupation of CB_1 and CB_2 receptors by agonist molecules: increased G protein affinity for GTP (and [^{35}S]GTPγS). The occupation of a CB_1 or CB_2 receptor by an agonist causes the α and βγ subunits of the heterotrimeric G protein to which it is coupled to dissociate and shifts the α subunit from a state in which it has higher affinity for GDP than GTP to one in which it has lower affinity for GDP than GTP. Once dissociated, the α and βγ subunits both act upon effectors until the GTP bound to the α subunit is dephosphorylated to GDP by the action of α subunit GTPase. The α and βγ subunit re-

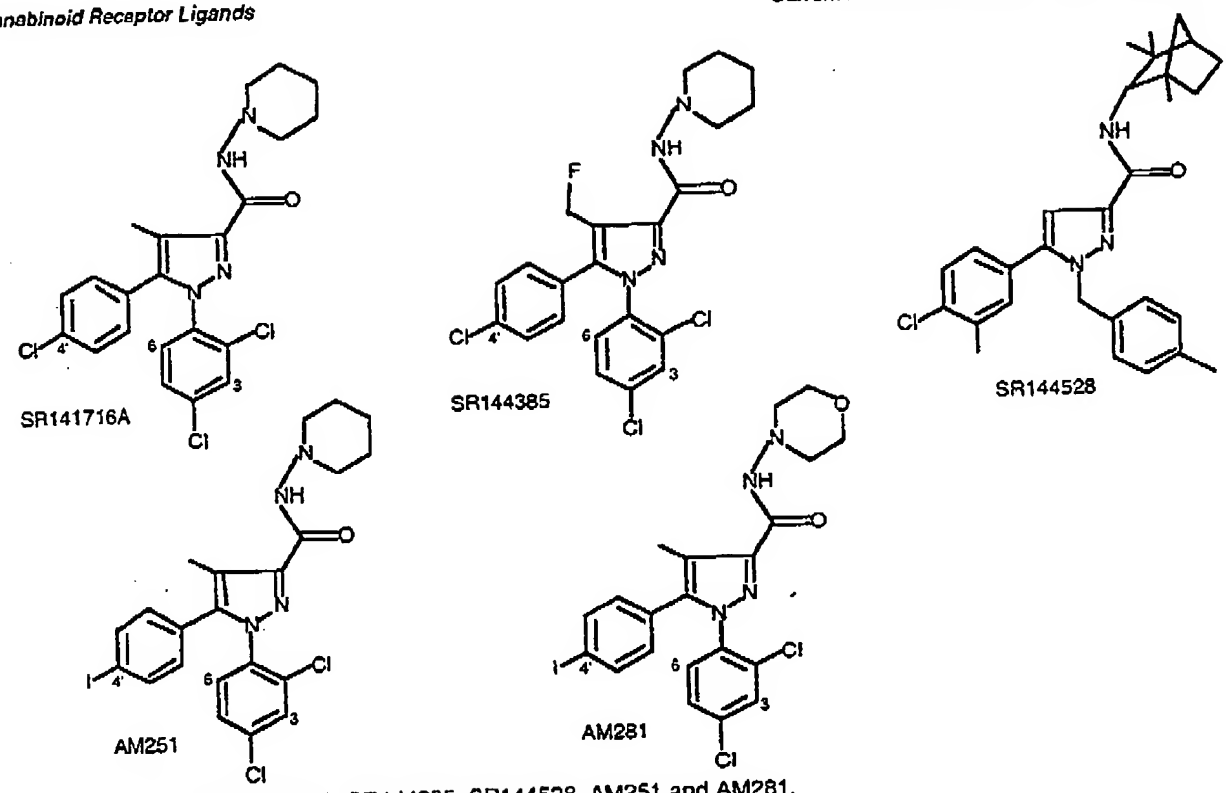

Fig. (5). Structures of SR141716A, SR144385, SR144528, AM251 and AM281.

associate and the reconstituted G protein is then ready for further activation by agonist. For an agonist to produce sufficient stimulation of [^{35}S]GTPγS membrane binding, it is important that the binding of [^{35}S]GTPγS that occurs in the absence of added agonist is minimized. This is achieved by adding high amounts of GDP and sodium chloride [55, 67, 69]. GDP decreases agonist-stimulated as well as basal binding of [^{35}S]GTPγS. However, it is the basal binding that it inhibits the more, the overall result being the production by GDP of concentration-related increases in net agonist-stimulated [^{35}S]GTPγS binding [67]. The amount by which GDP concentrations can be increased to enhance net agonist-stimulated [^{35}S]GTPγS binding is limited by the concentration-related inhibitory effect GDP has on absolute levels of basal and agonist-stimulated of binding. Thus, when GDP concentrations are progressively raised, a point is eventually reached at which [^{35}S]GTPγS binding has fallen to a level that is too low to be measured reproducibly [55].

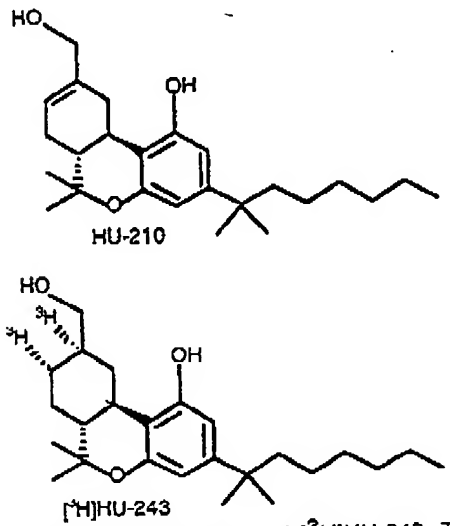

Fig. (6). Structures of HU-210 and [^{3}H]HU-243. The (+)-enantiomer of HU-210 is HU-211.

The other bioassay system exploits the negative coupling of CB_1 and CB_2 receptors to adenylate cyclase, the measured response usually being agonist-induced inhibition of forskolin-stimulated cyclic AMP production in cannabinoid receptor-containing tissue preparations (Tables 4 and 5). Although CB_1 or CB_2 transfected cells are now most frequently used to characterize novel cannabinoid receptor ligands with this assay, tissues that express CB_1 or CB_2 naturally have also been used. These include brain synaptosomes and primary cultures of central neurones or spleen cells (see above). Some information about the efficacy of ligands for CB_1 receptors has also been gleaned from a third bioassay that exploits the negative coupling of CB_1 (but not CB_2) receptors to N- and P/Q-type calcium channels [1]. In this case the measured response is agonist-induced inhibition of depolarization-stimulated inward calcium current in CB_1 receptor-containing tissue preparations (Table 6). However, this system is less suitable for routine use.

Table 3. Stimulatory Effect of Certain Cannabinoid Receptor Ligands on GTPγS Binding by Tissue or Cultured Cell Membranes Expressing Cannabinoid CB_1 or CB_2 Receptors

Preparation	Experimental Conditions	EC_{50} values (nM) and maximal degree of stimulation over basal (%)												
		CP559	CP552	CP505	THC	HU	(+)-WIN	(-)-WIN	AEA	Met	O-689	O-1054	CBN	Ref.
Human CB_1-transfected CHO cell membranes	0.1 nM [^{35}S]GTPγS; 50 µM GDP; 100 mM NaCl; 3 mM $MgCl_2$; 30 µg protein; 0.2 mM EGTA; 0.1% BSA; 60 min at 30°C (0.2 ml assay)	– ~40% by 20 nM	–	–	–	–	–	–	–	–	–	–	–	[59]
Human CB_1-transfected CHO cell membranes	0.1 nM [^{35}S]GTPγS; 50 µM GDP; 150 mM NaCl; 2.5 mM $MgCl_2$; 0.1% tissue; 1 mM EDTA; 0.25% BSA; 90 min at 30°C (1 ml assay)	–	–	–	–	–	473 78%	–	–	–	–	–	–	[60]
Human CB_1-transfected CHO cell membranes	0.1 nM [^{35}S]GTPγS; 50 µM GDP; 150 mM NaCl; 2.5 mM $MgCl_2$; 0.1% tissue; 1 mM EDTA; 0.25% BSA; 90 min at 30°C (1 ml assay)	–	–	–	–	–	360 77.9%	–	–	–	–	–	–	[63]
Human CB_1-transfected CHO cell membranes	1 nM [^{35}S]GTPγS; 320 µM GDP; 100 mM NaCl; 32 mM $MgCl_2$; 5 µg protein; 60 min at 37°C (0.25 ml assay)	18.6 103%	–	–	–	–	616.6 92%	–	–	–	–	–	>10 µM ~5%	[66]
Rat striatum membranes	0.05 nM [^{35}S]GTPγS; 20 µM GDP; 100 mM NaCl; 3 mM $MgCl_2$; 4 µg protein; 0.2 mM EGTA; 0.1 mg BSA; 60 min at 30°C (1 ml assay)	–	–	–	–	–	20 125%	–	–	–	–	–	–	[54]
Rat cerebellum membranes	0.05 nM [^{35}S]GTPγS; 30 µM GDP; 100 mM NaCl; 3 mM $MgCl_2$; 18 µg protein; 0.2 mM EGTA; 0.1% BSA; 60 min at 30°C (1 ml assay)	100 140%	–	800 167%	– 0%	–	180 182%	>10000 3%*	≥5100* –	–	–	–	–	[55]
Rat cerebellum membranes	0.05 nM [^{35}S]GTPγS; 20 µM GDP; 100 mM NaCl; 3 mM $MgCl_2$; 15 µg protein; 0.2 mM EGTA; 0.1 mg BSA; 60 min at 30°C (1 ml assay)	–	–	–	– 20%	–	120 270%	–	–	–	–	–	–	[19]
Rat cerebellum membranes	0.2 nM [^{35}S]GTPγS; 100 µM GDP; 1 mM $MgCl_2$; 15 µg protein; 1 mM EGTA; 0.25 mg BSA; 90 min at 30°C (0.5 ml assay)	9 100%	–	–	530 54%	–	99 75%	>10000	540* 73%	180 104%	–	–	170 30%	[62]
Rat cerebellum membranes	0.05 nM [^{35}S]GTPγS; 100 (or 10#) µM GDP; 150 mM NaCl; 9 mM $MgCl_2$ 10 µg protein; 0.2 mM EGTA; 1% BSA; 60 min (HU) or 30 min at 30°C (0.5 ml assay)	17.8 114% 61%#	0.47 165%	–	– 0% 51%#	0.55 140%	151 156% 89%#	–	– 0%	–	25.4 97%	246 60%	– 0%	[64]
Rat cerebellum membranes	0.2 nM [^{35}S]GTPγS; 100 µM GDP; 1 mM $MgCl_2$; 15 µg protein; 1 mM EGTA; 0.25 mg BSA; 90 min at 30°C (0.5 ml assay)	53 80%	–	–	216 54%	–	–	–	–	–	–	–	187 24%	[65]
Rat cerebellum membranes	0.05 nM [^{35}S]GTPγS; 30 µM GDP; 100 mM NaCl; 4-15 µg protein; 0.1% BSA; 120 min at 30°C (1 ml assay)	6.6 95%†	–	9 117%†	87 25%†	–	160 125%†	–	390* 82%†	320 79%†	–	–	–	[67]
Rat cerebellum membranes	0.65 nM [^{35}S]GTPγS; 10 µM GDP; 150 mM NaCl; 5 µg protein; 0.1% BSA; 30 min at 37°C	31 100%	–	–	–	–	120 117%	–	276* 66%	–	–	–	–	[46]
Rat cerebellum membranes	0.05 nM [^{35}S]GTPγS; 50 µM GDP; 100 mM NaCl; 5 mM $MgCl_2$; 40-50 µg protein; 0.1% BSA; 60 min at 30°C	100 145%	–	–	–	–	180 150%	–	–	330 148%	–	–	–	[45]

Preparation	Experimental Conditions	EC_{50} values (nM) and maximal degree of stimulation over basal (%)												Ref.
		CP559	CP552	CP505	THC	HU	(+)-WIN	(-)-WIN	AEA	Met	O-689	O-1054	CBN	
Rat (a) cerebellum (b) amygdala (c) hypothalamus membranes	0.05 nM [^{35}S]GTPγS; 30 μM GDP; 100 mM NaCl; 3 mM $MgCl_2$; 10-20 μg protein; 0.2 mM EGTA; 0.1% BSA at 30°C (1 ml assay)	-	-	-	-	-	(a) 156 (b) 84 (c) 131	-	-	-	-	-	-	[22]
Mouse whole brain membranes	0.1 nM [^{35}S]GTPγS; 50 μM GDP; 150 mM NaCl; 2.5 mM $MgCl_2$; 1 mM EDTA; 90 min at 30°C (1 ml assay)	-	-	-	-	-	~320*	-	-	-	-	-	-	[56]
Mouse whole brain membranes	0.1 nM [^{35}S]GTPγS; 50 μM GDP; 150 mM NaCl; 2.5 mM $MgCl_2$; 1 mM EDTA; 0.25% BSA; 90 min at 30°C	-	-	-	59* ~30%	-	347* ~150%	-	-	-	-	-	-	[57]
Mouse whole brain membranes	0.1 nM [^{35}S]GTPγS; 50 μM GDP; 150 mM NaCl; 2.5 mM $MgCl_2$; 1 mM EDTA; 0.25% BSA; 90 min at 30°C (1 ml assay)	61.7* 136%	-	-	70.9* 37%	2.25* 123%	-	-	845* 86%	-	-	-	-	[61]
Mouse whole brain membranes	0.1 nM [^{35}S]GTPγS; 100 μM GDP; 100 mM NaCl; 3 mM $MgCl_2$; 50 μg protein; 0.2 mM EDTA; 50 μg BSA; 60 min at 30°C (0.5 ml assay)	200 75%	-	-	-	-	-	-	-	-	-	-	-	[58]
Guinea-pig whole brain membranes	0.1 nM [^{35}S]GTPγS; 50 μM GDP; 150 mM NaCl; 2.5 mM $MgCl_2$; 1 mM EDTA; 90 min at 30°C (1 ml assay)	-	-	-	-	-	2960*	-	-	-	-	-	-	[58]
Human CB_2 transfected CHO cell membranes	1 nM [^{35}S]GTPγS; 320 μM GDP; 100 mM NaCl; 32 mM $MgCl_2$; 5 μg protein; 60 min at 37°C (0.25 ml assay)	2.75 42%	-	-	-	-	2.24 27%	-	-	-	-	-	575.4 -53%	[66]

* In the presence of 50 to 150 μM phenylmethylsulphonyl fluoride

- at 10 μM (-)-WIN55212

† Recalculated from normalized data, using 125% as the value for (+)-WIN55212 [67].

AEA, anandamide (Fig. 1); BSA, bovine serum albumin; CBN, cannabinol (Fig. 8); CHO, Chinese hamster ovary; CP559, CP55940 (Fig. 3); CP552, CP55244 (Fig. 3); O-689, fluoromethanandamide (Fig. 11); THC, Δ^9-THC (Fig. 1); HU, HU-210 (Fig. 6); CP505, CP50556 (Fig. 3); Met, methanandamide (Fig. 11); O-1054, 2,16,16-trimethyl-all-cis-5,8,11,14-docosatetraenoyl-2'-fluoroethanolamide (Fig. 11); THC, Δ^9-THC (Fig. 2); WIN, WIN55212 (Fig. 4).

The [^{35}S]GTPγS assay is the least sensitive of the three functional bioassays described in this section (Tables 3 to 6). Presumably this is because the cannabinoid receptor signal is less amplified in this assay, adenylate cyclase and calcium channels both being located further along the signalling cascade than G protein. The [^{35}S]GTPγS assay also differs from the other two assays in providing a total measure of G protein-mediated cannabinoid receptor activation rather than a measure of the activation of just one particular cannabinoid receptor effector mechanism. This assay should, therefore, be independent of any variations that may exist between tissues in the relative contribution made by different G protein-coupled effector mechanisms.

A measure of the relative efficacies of cannabinoid receptor agonists can be obtained in all three assay systems by constructing log dose response curves and then comparing the size of responses to maximal doses (E_{max} values). Indeed, there is usually no other way of obtaining an indication of the relative efficacies of cannabinoid receptor agonists from the existing published data. One exception to this is to be found in a paper by Burkey *et al.* [61] which contains relative efficacy values at CB_1 receptors for CP55940, 11-OH-Δ^8-THC-dimethylheptyl (HU-210), anandamide and Δ^9-THC estimated from [^{35}S]GTPγS binding data. It is noteworthy that the maximal effects of what appear to be full cannabinoid receptor agonists on forskolin-stimulated cyclic AMP production and on depolarization-stimulated inward calcium current usually fall well short of complete inhibition (Tables 4 to 6).

In the literature, and hence also in Tables 3 to 6, the potency of an agonist is usually expressed as the concentration (EC_{50}) of that agonist lying at the mid point of its log concentration-response curve. Caution should therefore be exercised in using these EC_{50} values to calculate relative potency values as (a) not all cannabinoid receptor agonists elicit the same maximal response in any given assay system (Tables 3 to 6) and (b) relative potency values should be calculated by comparing the concentrations of different drugs that elicit the same sized response. This point is well illustrated by the data of Burkey *et al.* [57] who reported

that Δ^9-THC has a 5.9 fold lower EC_{50} than (+)-WIN55212 in the [^{35}S]GTPγS binding assay. The EC_{50} of Δ^9-THC (59 nM) produced only about 15% stimulation of [^{35}S]GTPγS binding whereas the EC_{50} of (+)-WIN55212 (347 nM) produced about 75% stimulation. (+)-WIN55212 matched the half-maximal response to Δ^9-THC (15% stimulation) at a concentration of about 25 nM, showing it to be more than twice as potent as Δ^9-THC in this assay.

Table 4. Inhibitory Effect of Certain Cannabinoids on Cyclic AMP Production by Cultured Cells Expressing Cannabinoid CB_1 Receptors or by Brain Tissue Stimulated by Forskolin (FSK), Secretin, Prostaglandin E_1, Prostacyclin or Isoprenaline

Preparation	Mode of cyclic AMP stimulation	Inhibitory EC_{50} values (nM) and maximal degree of inhibition (%)												
		CP559	CP552	CP505	THC	HU	Nab	(+)-WIN	(-)-WIN	AEA	2-AG	PEA	CBN	Ref.
Human CB_1-transfected CHO cells	0.5 μM FSK	0.99 80%	0.128 80%	–	13 ~40%	–	–	–	–	–	–	–	–	[77]
Human CB_1-transfected CHO cells	0.5 μM FSK	–	–	–	–	–	–	–	–	160 ~100%	–	>1 mM 0% at 1 mM	–	[81]
Human CB_1-transfected CHO cells	FSK	1.27	–	–	–	–	–	–	–	–	–	–	–	[30]
Human CB_1-transfected CHO cells	FSK	1.83	–	–	16.5	0.197	–	24	–	322	–	–	>1 μM 0% at 1 μM	[32]
Human CB_1-transfected CHO cells	FSK	1.2	–	–	10	–	–	14	–	–	–	–	–	[89]
Human CB_1-transfected 293 cells	FSK	3.1 ~45%	–	–	–	0.19 ~55%	–	7.6 ~40%	>1 μM 0% at 1 μM	81.6 ~75%	–	–	–	[16]
Human CB_1-transfected CHO cells	3 μM FSK	0.16 ~75%	–	–	2.25 ~75%	–	–	17.95 ~75%	–	–	–	–	–	[59]
Human CB_1-transfected CHO cells	3 μM FSK	2 ~83%	–	–	10.7 ~60%	–	–	44.3 ~60%	–	108.5 ~29%	–	–	–	[91]
Human CB_1-transfected CHO cells	1 μM FSK	4 62%	–	–	–	–	–	31 75.1%	–	–	–	–	–	[24]
Human CB_1-transfected CHO cells	3 μM FSK	2 75%	–	–	–	–	–	–	–	–	–	–	–	[43]
Human CB_1-transfected 293 cells	0.5 μM FSK	4.17 69%	–	–	–	–	–	1.64 63%	–	–	–	–	–	[93]
CB_1-transfected COS cells	1 μM FSK	–	–	–	–	–	–	–	–	–	428 ~80%	–	–	[44]
Rat CB_1-transfected CHO cells	0.5 μM FSK	0.87 ~60%	–	–	13.5 ~40%	–	16.8 ~60%	–	–	–	–	–	– ~12% at 1 μM	[75]
Rat CB_1-transfected CHO cells	–	1.8	0.2	2.4	55	0.02	3.1	24	>2000	–	–	–	–	[78]
Rat CB_1-transfected CHO cells	1 μM FSK	–	–	–	9.1 ~45%	0.8 50-55%	–	–	–	201 35-40%	–	>10 μM 0% at 0.1nM to 10 μM	–	[80]
Rat CB_1-transfected CHO cells	PGE_1	–	–	–	9.2 ~45%	–	–	–	–	100.5 ~60%	–	–	–	[66]
Rat CB_1-transfected COS cells	1 μM FSK	–	–	–	13 62%	–	–	–	–	–	–	–	–	[34]
Rat CB_1-transfected COS cells	1 μM FSK	–	–	–	11	0.035	–	–	–	–	–	–	120	[41]
Human U373 MG astrocytoma cells	5 μM FSK	0.8 ~100%	–	–	–	–	–	32 ~100%	–	–	–	–	–	[66]
Mouse N18TG2 cell membranes	1 μM FSK#	–	–	~100 ~32%	~220 ~29%	–	–	–	–	–	–	–	~500 ~9%	[70]
Mouse N18TG2 cell membranes	100 μM secretin	–	–	–	530 ~30%	–	–	–	–	–	–	–	1400 ~14%	[72]
Mouse N18TG2 cell membranes	0.5 μM secretin	25 35%	5 35%	100	430	–	–	–	–	–	–	–	–	[73]
Mouse N18TG2 cell membranes	0.5 μM secretin	–	–	–	–	7.2 (29%)	–	–	–	–	–	–	–	[74]
Mouse N18TG2 cells	1 μM FSK	–	–	–	–	2.9 ~60%	–	–	–	540 ~40%	–	>10 μM 0% at 0.1nM to 10 μM	–	[90]
Mouse N18TG2 cell membranes	0.65 μM secretin	–	–	–	–	–	–	–	–	1000 45%	–	–	–	[84]

(Table 4). contd....

Preparation	Mode of cyclic AMP stimulation	Inhibitory EC_{50} values (nM) and maximal degree of inhibition (%)												Ref.
		CP559	CP552	CP505	THC	HU	Nab	(+)-WIN	(-)-WIN	AEA	2-AG	PEA	CBN	
Mouse N18TG2 cells	1 μM prostacyclin	-	-	- 50% at 30 μM	- 30% at 30 μM	-	-	-	-	-	-	-	-	[71]
Mouse N18TG2 cells	0.5 μM secretin	-	-	-	-	1.8 63%	-	-	-	-	-	-	-	[74]
Mouse N18TG2 cells	1 μM FSK	-	-	-	1.2 -35%	-	-	-	-	-	-	-	-	[85]
Mouse N18TG2 cells	1 μM FSK	-	-	-	35 45%	-	-	-	-	-	-	-	-	[34]
Mouse NG108-15 cells	1 μM FSK	-	-	-	-	-	16.2 35.6%	-	-	-	-	-	-	[87]
SH-SY5Y cells	1 μM FSK	-	-	-	-	-	20.2 45.4%	-	-	-	-	-	-	[87]
Rat cortical neurones (primary culture)	3 μM FSK	-	-	-	-	-	-	-	-	1200 >30%	800 >40%	-	-	[92]
Rat cortical neurones (primary culture)	1 μM FSK	4.6 54%	-	-	-	-	-	85 73%	-	-	-	-	-	[18]
Rat cortical neurones (primary culture)	1 μM isoprenaline	1 38%	-	-	-	-	-	5.1 58%	-	-	-	-	-	[18]
Rat cerebellar neurones (primary culture)	1 μM FSK	1.9	-	-	-	-	-	-	-	-	-	-	-	[18]
Rat cerebellar granule cells (primary culture)	1 μM FSK	220 65%	-	130 65%	2400 60%	-	-	410 46%	>10 μM <10% at 111 nM to 111 μM	-	-	-	-	[79]
Rat cerebellar membranes	None (basal)	60 40%	-	-	-	-	-	100 41%	-	1900 33%	-	-	-	[82]
Rat cerebellar membranes	None (basal)	-	-	200 40%	-	-	-	100 40%	-	-	-	-	-	[79]
Rat cerebellar membranes	FSK or basal	-	-	-	-	-	-	320 32%	>10 μM	-	-	-	-	[76]
Rat striatal membranes	FSK or basal	-	-	-	-	-	-	400 28%	-	-	-	-	-	[76]
Rat striatal neurones (primary culture)	1 μM FSK	3.5 -40%	-	-	-	-	-	-	-	-	-	-	-	[18]
Rat cerebellar membranes	None (basal)	150 32%	-	-	-	-	-	210 35%	-	-	-	-	-	[63]
Rat striatal membranes	None (basal)	310 25%	-	-	-	-	-	200 29%	-	-	-	-	-	[83]
Rat substantia nigra membranes	FSK	-	-	-	-	-	-	40 35%	-	-	-	-	-	[30]
Mouse cerebellum membranes	1 μM FSK	72 35%	-	-	-	-	-	-	-	-	-	-	-	[90]

* In the presence of 10 to 200 μM phenylmethylsulphonyl fluoride.
# Effects of cannabinoids on secretin-stimulated cAMP production also investigated [70].
AEA, anandamide (Fig. 1); 2-AG, 2-arachidonoyl glycerol (Fig. 1); CBN, cannabinol (Fig. 8); CHO, Chinese hamster ovary; CP559, CP55940 (Fig. 3); CP552, CP55244 (Fig. 3); HU, HU-210 (Fig. 6); CP505, CP50556 (Fig. 3); Nab, nabilone (Fig. 2); PEA, palmitoylethanolamide (Fig. 1); THC, Δ^9-THC (Fig. 2); WIN, WIN55212 (Fig. 4).

Some cannabinoid receptor agonists have relatively low CB_1 and/or CB_2 efficacies. The pharmacological properties of such 'efficacy-driven' agonists is expected to show a particularly strong tissue-dependence. In a tissue preparation that contains a high concentration of cannabinoid receptors so that there is a significant 'receptor reserve', the size of the maximal response to an efficacy-driven agonist may be the same as that to a high-efficacy (affinity-driven) agonist, giving the false impression that both compounds have the same (high) efficacy. On the other hand, in a tissue preparation containing far fewer cannabinoid receptors (no 'receptor reserve'), the same efficacy-driven agonist may behave as a partial agonist or antagonist (e.g. see O-823 in next section). Hence if the relative efficacies of cannabinoid receptor agonists are determined by comparing maximal response size, it is important that this has been done using data obtained in the same tissue preparation and that the receptor population of this preparation (a) is small enough so that there is no significant receptor reserve, yet (b) is large enough to detect responses to low-efficacy compounds. Other reasons for using the same tissue preparation to determine the relative efficacies of cannabinoid receptor agonists are firstly, that there may be intertissue variations in the abilities of CB_1 or CB_2 receptors to amplify agonist-receptor interactions and secondly, that some tissues may

contain CB_1 or CB_2 receptor subtypes with their own distinct recognition sites or effector mechanisms. Already there is evidence that the efficiency with which G proteins transduce the agonist-cannabinoid receptor interaction can vary, at least within the brain. Thus there are several reports that the efficiency of coupling of cannabinoid receptors to G proteins, as defined for example by the ratio of apparent B_{max} of maximal cannabinoid receptor-stimulated [^{35}S]GTPγS binding to cannabinoid receptor B_{max}, is not the same in all brain areas [19, 22, 55, 69]. Indeed, there seem to be some brain areas, for example hypothalamus, that contain cannabinoid receptors with high coupling efficiency but in low concentration and other brain areas, for example hippocampus, that contain cannabinoid receptors with low coupling efficiency but in high concentration [22]. Consequently, the responsiveness of different brain areas to high-efficacy (affinity-driven) and low-efficacy (efficacy-driven) agonists may not always be highest in brain areas that contain the most cannabinoid receptors. Cannabinoid receptor coupling efficiency may also be affected by prior exposure to cannabinoids [19].

In the [^{35}S]GTPγS assay, increases in GDP concentration seem to magnify differences between the efficacies of different agonists such that the optimal GDP concentration appears to be higher for the assay of high-efficacy than low-efficacy agonists [67]. Indeed, elevating the concentration of GDP may completely abolish the ability of a low efficacy agonist to increase [^{35}S]GTPγS binding above basal levels. Compare for example the activities of the high-efficacy agonist, (+)-WIN55212 and the lower efficacy agonist Δ^9-THC observed in this assay by Griffin *et al.* [64]. Whereas (+)-WIN55212 produced greater stimulation of [^{35}S]GTPγS binding (over basal) at 100 μM GDP than at 10 μM GDP, Δ^9-THC stimulated [^{35}S]GTPγS binding in the presence of 10 μM GDP but not 100 μM GDP.

Cannabinoid Receptor Ligands

Classical Cannabinoids

The best known member of this group is Δ^9-tetrahydrocannabinol (Δ^9-THC) (Fig. 2). This is the main psychotropic constituent of cannabis and like all classical cannabinoids, it is a dibenzopyran derivative. Δ^9-THC undergoes significant binding to cannabinoid receptors at submicromolar concentrations, with similar affinities for CB_1 and CB_2 receptors (Table 2). At CB_1 receptors, Δ^9-THC behaves as an affinity-driven agonist, the sizes of its maximal effects in several CB_1 receptor-containing tissue preparations falling well below those of higher efficacy cannabinoid receptor agonists such as CP55940 and (+)-WIN55212 (Tables 3 and 4). As is to be expected for an affinity-driven agonist, the efficacy of Δ^9-THC shows 'tissue-dependence', there being some CB_1 bioassay systems in which it can elicit maximal responses that match those of higher efficacy agonists (Table 4). Δ^8-THC (Fig. 7), which has affinities for CB_1 and CB_2 receptors that are similar to those of Δ^9-THC (Table 2), also behaves as an affinity-driven agonist at CB_1 receptors [75, 77]. As to the CB_2 efficacy of Δ^9-THC, this is even less than at CB_1 receptors (Tables 4 and 5). Indeed, in some investigations Δ^9-THC has failed to show any agonist activity at all at CB_2 receptors and, in one set of experiments performed with CHO cells transfected with human CB_2 receptors and using the cyclic AMP assay, it behaved as a CB_2 receptor antagonist [34]. There are also some reports that Δ^9-THC behaves as an antagonist at the CB_1 receptor both in the [^{35}S]GTPγS

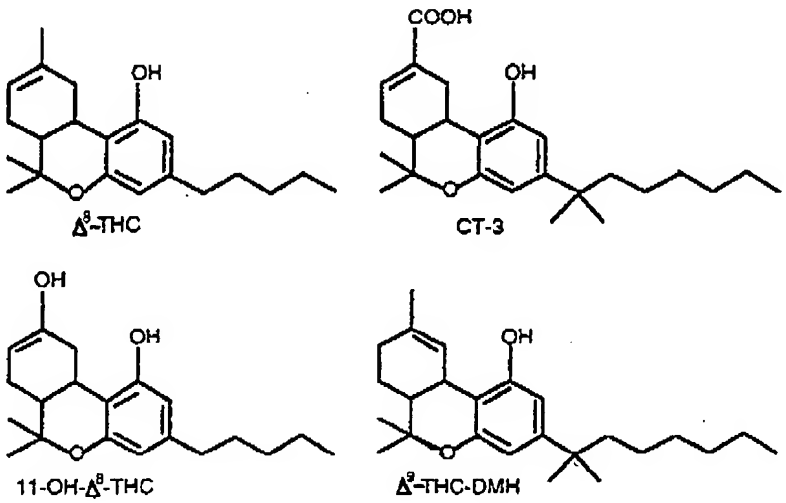

Fig. (7). Structures of four classical cannabinoids (DMH, dimethylheptyl).

assay performed with rat cerebellar membranes [19, 64] and when the measured response is (+)-WIN55212-induced inhibition of glutamatergic synaptic transmission in rat cultured hippocampal neurones [102].

Two other plant cannabinoids, cannabinol and cannabidiol (Fig. 8), have less affinity for cannabinoid receptors than Δ^8- or Δ^9-THC (Table 2). At CB_1 receptors, cannabinol behaves as an affinity-driven agonist with even less efficacy than Δ^9-THC (Tables 3 and 4). There is also one report that it behaves as an agonist for CB_2 receptors in the cyclic AMP assay [41]. However, in the GTPγS assay, cannabinol has been found to exhibit the properties of an inverse agonist for CB_2 receptors (Table 7). (The concept of inverse agonism is discussed later). Cannabidiol lacks significant agonist activity, at least at CB_1 receptors, as

Table 5. Inhibitory Effect of Certain Cannabinoids on Forskolin-stimulated Cyclic AMP Production by Cultured Cells Expressing Cannabinoid CB_2 Receptors

Preparation	Forskolin (μM)	Inhibitory EC_{50} values (nM) and maximal degree of inhibition (%)								Ref.
		CP559	THC	HU	(+)-WIN	(−)-WIN	AEA	2-AG	CBN	
Human CB_2-transfected CHO cells	?	2.51	–	–	–	–	–	–	–	[30]
Human CB_2-transfected CHO cells	5	0.72 −55%	– 0%	0.37 −50%	0.63 −45%	>1 μM 0% at 1 μM or less	– 0%	–	–	[12]
Human CB_2-transfected CHO cells	?	2.89	41.8	0.578	0.407	–	957	–	>1 μM	[32]
Human CB_2-transfected CHO cells	1	–	>1 μM 0% at 0.01 to 1000 nM	1 −48%	–	–	>1 μM* 0% at 0.01 to 1000 nM	–	–	[14]
Human CB_2-transfected COS cells	1	–	>1 μM <10% at 1 to 1000 nM	–	–	–	–	–	–	[34]
Human CB_2-transfected CHO cells	5	2 −80%	–	–	3 −75%	–	–	–	–	[94]
Human CB_2-transfected COS cells	1	–	>1 μM 21% at 1 μM	0.078	–	–	–	–	261	[41]
Human CB_2-transfected CHO cells	3	2.51 90%	–	–	–	–	–	–	–	[43]
Human CB_2-transfected 293 cells	0.5	52.1 80%	–	–	12.3 80%	–	–	–	–	[93]
Human CB_2-transfected CHO cells	3	– 76% at 100 nM	– 45% at 100 nM	–	– 80% at 100 nM	–	– 38% at 1 μM	–	–	[35]
Mouse CB_2-transfected CHO cells	3	– 75% at 100 nM	– 63% at 100 nM	–	– 62% at 100 nM	–	– 64% at 1 μM	–	–	[35]
CB_2-transfected COS cells	1	–	–	–	–	–	–	784* −60%	–	[44]

* In the presence of 150 or 200 μM phenylmethylsulphonyl fluoride.
AEA, anandamide (Fig. 1); 2-AG, 2-arachidonoyl glycerol (Fig. 1); CBN, cannabinol (Fig. 8); CHO, Chinese hamster ovary; CP559, CP55940 (Fig. 3); HU, HU-210 (Fig. 6); THC, Δ^9-THC (Fig. 2); WIN, WIN55212 (Fig. 4).

Table 6. Inhibitory Effect of Cannabinoids on Voltage-activated Calcium Currents in Membranes of Cultured Cells Expressing Cannabinoid CB_1 Receptors

Preparation	Agonist	Agonist concentration (nM)	EC_{50} (nM)	Inhibition (%)	Ref
AtT-20 cells transfected with human CB_1 receptors	(+)-WIN55212	100	–	12% by 100 nM	[32]
AtT-20 cells transfected with rat CB1 receptors	(+)-WIN55212 Anandamide	1 to 300† 300	11 –	38% (Emax) 34% by 300 nM	[13]
Rat superior cervical ganglion cultured neurones transfected with rat CB_1 receptors	(+)-WIN55212 CP55940 Anandamide	1 to 3000† 1 to 10000 100	47 7 –	73% (Emax) 38% (Emax) 0 to 40% by 100 nM	[99]
NG108-15 neuroblastoma-glioma cells	Δ^9-THC CP55940	30 µM† 1 µM†	– –	40% 40%	[96]
NG108-15 neuroblastoma-glioma cells	(+)-WIN55212 CP55940	1 to 1000† 100	~3 –	43% (Emax) 36% by 100 nM	[95]
N18 neuroblastoma cells	(+)-WIN55212 Anandamide	100 1 to 1000†	– 20	54% by 100 nM 33% (Emax)	[97]
N18 neuroblastoma cells	(+)-WIN55212 Anandamide	~3 to 100 ~10 to 300	~10 ~10	~43% (Emax) ~30% (Emax)	[81]
N18 neuroblastoma cells	Mead ethanolamide	30 to 1000	124	~60% (Emax)	[98]
Rat hippocampal cultured neurones	(+)-WIN55212 (+)-WIN55212 CP55940 Anandamide	1 to 300 100*† 100 300	21 – – –	33% (Emax) 29.5% by 100 nM 25.5% by 100 nM 28.6% by 300 nM	[100]
Rat hippocampal	(+)-WIN55212	30 to 3000*	14	~23% (Emax)	[101]

cultured neurones should be in Table
*Antagonized by 200 or 300 nM SR141716A.
†Pertussis toxin sensitive.
Mead ethanolamide, 5Z, 8Z, 11Z-eicosatrienoic acid.

do cannabichromene and cannabigerol, also both plant cannabinoids. A high concentration (10 µM) of each of these three compounds failed to inhibit secretin-stimulated cyclic AMP production by N18TG2 cell membranes [72]. There is also a report that 10 µM cannabidiol does not enhance [^{35}S]GTPγS binding to rat cerebellar membranes [65]. Instead it was found to antagonize the stimulatory effect of CP55940 in this assay. Under the same conditions, 10 µM cannabinol did not antagonize CP55940 [65].

The affinities of Δ^9-THC, cannabinol, 11-hydroxy-Δ^8-THC and 11-hydroxy-cannabinol for cannabinoid receptors can be markedly enhanced by increasing the length of the alkyl side chain and by introducing methyl substituents into the lengthened side chain to produce dimethylheptyl analogues of these compounds (Table 2 and Figs. 6 to 8). These affinity increases are not accompanied by any marked changes in relative affinity for CB_1 and CB_2 receptors. The same changes in the alkyl side chain also enhance CB_1 and CB_2 receptor functional potency and efficacy. For example, in contrast to Δ^8-THC [75, 77], 11-OH-Δ^8-THC-dimethylheptyl (HU-210) has E_{max} values at CB_1 receptors that approximate to those of the high-efficacy cannabinoid receptor agonist, CP55940 (Tables 3 and 4). Unlike Δ^8-THC, HU-210 contains an 11-OH group. However, there is no evidence that insertion of this group produces any notable efficacy increase. Thus although 11-OH-Δ^8-THC is about 2 times more potent than Δ^8-THC as an inhibitor of secretin-stimulated cyclic AMP production in N18TG2 cell membranes, the maximal degree of inhibition produced by the two compounds is the same [72]. Similarly, in [^{35}S]GTPγS binding assays performed with rat cerebellar membranes, whilst 11-OH-Δ^9-THC is more potent than Δ^9-THC, the two compounds each elicit maximal stimulatory responses of about the same size [62]. The dimethylheptyl and 11-OH-dimethylheptyl analogues of cannabinol are also potent CB_1 and CB_2 receptor agonists. Their EC_{50} values for inhibition of forskolin-stimulated cyclic AMP production are 0.18 and 0.056 nM respectively in CHO cells stably transfected with rat CB_1 receptors and 0.79 and 0.208 nM respectively in CHO cells stably transfected with human CB_2 receptors [41]. The corresponding EC_{50} values for cannabinol are 120 and 261 nM respectively [41]. Whether these dimethylheptyl and 11-OH-dimethylheptyl analogues have greater efficacy than cannabinol remains to be announced. It has been reported, however, that 11-OH-cannabinol has negligible agonist activity at CB_2 receptors [41].

The degree of rigidity of the alkyl side chain also seems to have pharmacological importance, there being evidence that the introduction of a carbon-carbon triple bond into this part of the molecule reduces efficacy at CB_1 and CB_2 receptors without

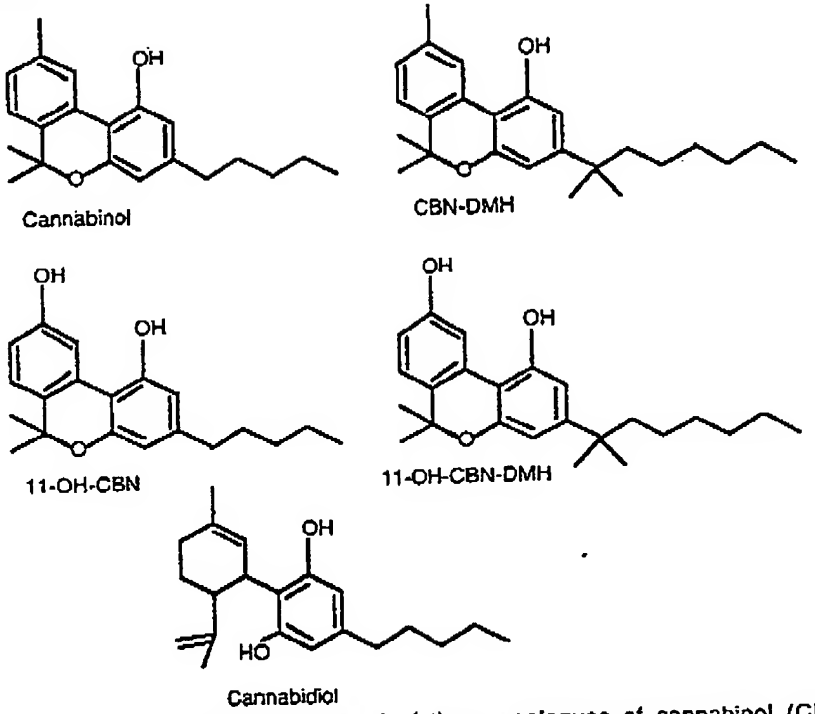

Fig. (8). Structures of cannabinol and cannabidiol and of three analogues of cannabinol (CBN, cannabinol; DMH, dimethylheptyl).

decreasing affinity for these receptor types [26, 36, 49, 103]. Thus 6'-azidohex-2'-yne-Δ^8-THC (O-1184; Fig. 9) has greater affinity than Δ^8-THC for both CB_1 and CB_2 receptors (Table 2). Yet, it behaves as a weak inverse agonist at CB_2 receptors [49] and, at CB_1 receptors, may have even lower efficacy than Δ^8-THC, behaving as a partial agonist in one assay system (inhibition of forskolin-stimulated cyclic AMP production by CHO cells transfected with human CB_1 receptors [49]) and as an antagonist in another [26]. A second classical cannabinoid with a 3-bond ynyl-containing side chain that seems to have high cannabinoid receptor affinity but reduced efficacy is 6'-cyanohex-2'-yne-Δ^8-THC (O-823; Fig. 9). The K_i value of this compound for displacement of [^{3}H]CP55940 from CB_1 binding sites is 0.77 nM. However, whilst it behaves as a potent cannabinoid receptor agonist in one CB_1-containing bioassay system (the mouse isolated vas deferens preparation), in another it behaves as a potent antagonist (myenteric plexus-longitudinal muscle preparation of guinea-pig small intestine) [104]. Using tissue obtained from Δ^9-THC-tolerant mice, it became possible to demonstrate O-823-induced antagonism of a cannabinoid receptor agonist in the vas deferens as well, suggesting that like O-1184, O-823 is a potent affinity-driven cannabinoid receptor agonist and that it behaves as an agonist in tissues in which cannabinoid receptors are present in relatively high concentrations and/or have relatively efficient coupling to their second messenger system (the vas deferens) and as an antagonist in tissues in which these receptors are present at lower concentrations and/or are less efficiently coupled (myenteric plexus-longitudinal muscle preparation and cannabinoid tolerant vas deferens).

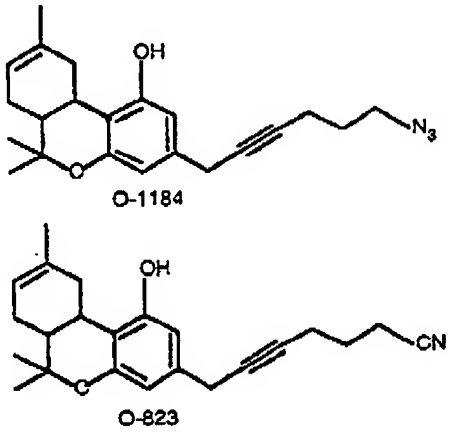

Fig. (9). Structures of O-1184 and O-823.

The results obtained with ynyl compounds such as O-1184 and O-823 provide clues as to how the structural features of classical cannabinoids that govern affinity for CB_1 and CB_2 receptors differ from those that determine efficacy at these receptors. So too do data obtained from experiments with the dimethylheptyl analogue of Δ^8-THC-11-oic acid (CT-3; Fig. 7) using CHO or COS cells transfected with rat CB_1 or human CB_2 receptors [41]. These experiments showed CT-3 to have about 8 times greater functional potency at the

Table 7. Inhibitory Effect of Certain Cannabinoid Receptor Ligands on GTPγS Binding by Tissue or Cultured Cell Membranes Expressing Cannabinoid CB_1 or CB_2 Receptors

Preparation	Experimental Conditions	EC_{50} values (nM) and maximal degree of inhibition relative to basal (%)				
		SR141	SR144	AM630	CBN	Ref.
Human CB_1-transfected CHO cell membranes	0.1 nM [^{35}S]GTPγS; 50 μM GDP; 100 mM NaCl; 3 mM $MgCl_2$; 30 μg protein; 0.2 mM EGTA; 0.1% BSA; 60 min at 30°C (0.2 ml assay)	– -25% by 100 nM	–	–	–	[59]
Human CB_1-transfected CHO cell membranes	0.1 nM [^{35}S]GTPγS; 50 μM GDP; 150 mM NaCl; 2.5 mM $MgCl_2$; 0.1% tissue; 1 mM EDTA; 0.25% BSA; 90 min at 30°C (1 ml assay)	0.82* 22.3%	–	–	–	[60]
Human CB_1-transfected CHO cell membranes	0.1 nM [^{35}S]GTPγS; 50 μM GDP; 150 mM NaCl; 2.5 mM $MgCl_2$; 0.1% tissue; 1 mM EDTA; 0.25% BSA; 90 min at 30°C (1 ml assay)	–	–	900* 20.9%	–	[63]
Human CB_1-transfected CHO cell membranes	1 nM [^{35}S]GTPγS; 320 μM GDP; 100 mM NaCl; 32 mM $MgCl_2$; 5 μg protein; 60 min at 37°C (0.25 ml assay)	5.5 47%	–	–	–	[66]
Rat cerebellum membranes	0.2 nM [^{35}S]GTPγS; 100 μM GDP; 1 mM $MgCl_2$; 15 μg protein; 1 mM EGTA; 0.25 mg BSA; 90 min at 30°C (0.5 ml assay)	>10 μM slight inhibition at 10 μM	–	–	–	[62]
Mouse whole brain membranes	0.1 nM [^{35}S]GTPγS; 50 μM GDP; 150 mM NaCl; 2.5 mM $MgCl_2$; 1 mM EDTA; 90 min at 30°C (1 ml assay)	–	–	>0.1 mM* ~0%†	–	[56]
Guinea-pig whole brain membranes	0.1 nM [^{35}S]GTPγS; 50 μM GDP; 150 mM NaCl; 2.5 mM $MgCl_2$; 1 mM EDTA; 90 min at 30°C (1 ml assay)	–	–	>0.1 mM* ~0%†	–	[58]
Human CB_2-transfected CHO cell membranes	1 nM [^{35}S]GTPγS; 320 μM GDP; 100 mM NaCl; 32 mM $MgCl_2$; 5 μg protein; 60 min at 37°C (0.25 ml assay)	1000 65%	–	–	575.4 53%	[66]
Human CB_2-transfected CHO cell membranes	0.1 nM [^{35}S]GTPγS; 20 μM GDP; 100 mM NaCl; 10 mM $MgCl_2$; 20 μg protein; 0.2 mM EDTA; 90 min at 30°C (0.5 ml assay)	–	10.4 49%	76.6 47%	–	[47]

* In the presence of 100 μM phenylmethylsulphonyl fluoride.
† At 100 μM AM630.
BSA, bovine serum albumin; CBN, cannabinol (Fig. 8); CHO, Chinese hamster ovary; SR141, SR141716A (Fig. 5); SR144, SR144528 (Fig. 5). See Fig. 13 for the structure of AM630.

CB_2 than the CB_1 receptors, when the measured response is inhibition of forskolin-stimulated cyclic AMP production (EC_{50} = 116.2 and 927 nM respectively), but about 5 times greater binding potency at the CB_1 than the CB_2 receptors (Table 2).

Several CB_2-selective classical cannabinoids have now been developed (Fig. 10) [33, 38]. Huffman *et al.* [38] discovered that whilst removal of the phenolic OH group from HU-210 to form 1-deoxy-11-OH-Δ^8-THC-dimethylheptyl (JWH-051) did not significantly affect affinity for CB_1 receptors, it greatly enhanced CB_2 receptor affinity (Table 2). As a result, JWH-051 was found to have 37.5 fold selectivity for CB_2 receptors. Even more dramatic is the CB_2-selectivity shown in binding experiments by JWH-133 and JWH-139 and by the Merk-Frosst compounds, L759633 and L759656 (Table 2). The CB_2 receptor affinity of JWH-139, L759633 and L759656 is somewhat less than that of JWH-051 or JWH-133, although still in the low nM

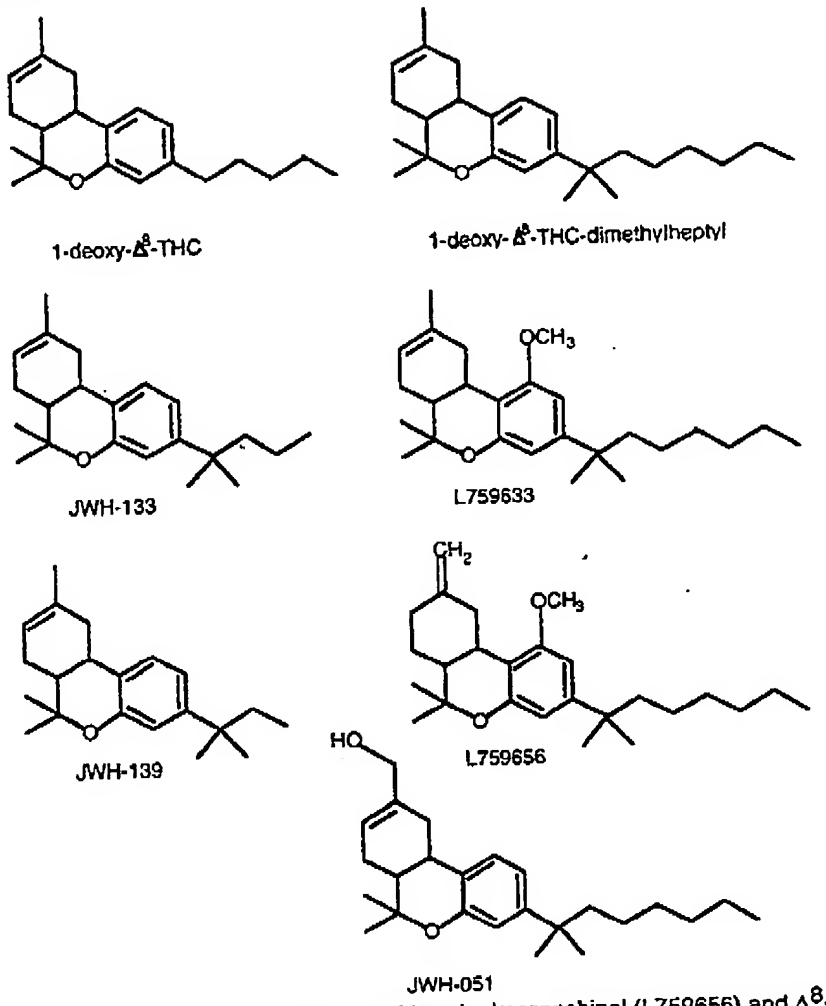

Fig. (10). Structures of some deoxy or methoxy analogues of hexahydrocannabinol (L759656) and Δ^8-THC.

range. More important, however, is the very much lower affinity JWH-133, JWH-139 and the two Merk-Frosst compounds have for CB_1 receptors than JWH-051. L759633 and L759656 seem to be CB_2 receptor agonists with both high efficacy and high potency. Thus Ross *et al.* [47] have reported firstly, that each of these compounds is approximately equipotent with the high-efficacy cannabinoid receptor agonist, CP55940, in inhibiting forskolin-stimulated cyclic AMP production by human CB_2 receptor transfected CHO cells and secondly, that the maximum degree of inhibition produced in this assay by all three compounds is the same. They found L759656 (10 μM) to be inactive at CB_1 receptors and L759633 to behave as a weak CB_1 receptor agonist with an EC_{50} of about 10 μM. Although there is good evidence from in vivo experiments that JWH-051 is a potent CB_1 receptor agonist [38] there are no reports as to whether it is also a CB_2 receptor agonist. Whether it will prove possible to develop agonists from classical cannabinoids that exhibit the same high degree of selectivity for CB_1 receptors that the Merk-Frosst compounds show for CB_2 receptors remains to be established.

Finally, for Δ^8-THC, Δ^9-THC and other classical cannabinoids with chiral centres, it is the (−)-enantiomers that show the greater CB_1 and CB_2 receptor affinity and functional potency [1]. This stereoselectivity is well illustrated by comparing the CB_1 or CB_2 affinities of (−)- and (+)-11-OH-dimethylheptyl-Δ^8-THC (HU-210 and HU211 respectively) (Table 2) or their potencies in CB_1 and CB_2 receptor-containing bioassay systems [12, 74, 105].

Non-classical Cannabinoids

This group of cannabinoids was developed by a Pfizer research team [106]. It consists of bicyclic and tricyclic analogues of Δ^9-THC that lack a pyran ring. A particularly important member of this group of compounds is the cannabinoid receptor agonist, CP55940 (Fig. 3) as it is the tritiated form of this compound that was used to demonstrate for the first time that brain tissue contains specific cannabinoid binding sites [107]. It was this landmark observation in particular that led to the realization that cannabinoids

act through receptors. CP55940 binds equally well to CB_1 and CB_2 receptors (Table 2). It shows high affinity for both receptor types, explaining the usefulness of radiolabelled CP55940 as a probe for CB_1 and CB_2 receptors. CP55940 behaves as an efficacy-driven agonist for both receptor types, the sizes of the effects it produces at maximal concentrations in CB_1 and CB_2 receptor assay systems often matching or exceeding the maximal responses to several other cannabinoid receptor agonists (Tables 3 to 5). Evidence that CP55940 does not need to occupy all cannabinoid receptors in the cerebellum to elicit a maximal response lends further support to its classification as a high-efficacy agonist [90]. Other non-classical cannabinoids often used as experimental tools are CP55244 and CP50556 (L-nantradol) (Fig. 3), and desacetyl-L-nantradol [1]. These also behave as high-affinity, high-efficacy agonists, at least for CB_1 receptors (Tables 3 and 4 and [1]). Indeed, CP50556 and CP55244 may have even higher CB_1 efficacy than CP55940 (Table 3 and [67]). It seems likely that these other non-classical cannabinoids share the ability of CP55940 to interact with CB_2 receptors. However, this remains to be established. Like classical cannabinoids, non-classical cannabinoids with chiral centres exhibit significant stereoselectivity, the (–)-enantiomers having the greater activity (Table 2 and [1]).

Eicosanoids

The prototypic member of the eicosanoid group of cannabinoid receptor agonists is arachidonoylethanolamide (anandamide) (Fig. 1). This is the first of four endogenous cannabinoid receptor agonists to have been discovered in mammalian brain and other tissues, the others being 2-arachidonoyl glycerol, homo-γ-linolenoylethanolamide and docosatetraenoylethanolamide [1, 2, 5, 108]. Of these, the most investigated and probably also the most important physiologically, are anandamide and 2-arachidonoyl glycerol.

Anandamide and Related Fatty Acid Amides

Anandamide binds significantly to both types of cannabinoid receptor with marginally higher affinity for the CB_1 receptor (Table 2). Indeed, when protected from hydrolysis (see below), its affinity for CB_1 receptors matches that of Δ^9-THC. Anandamide also resembles Δ^9-THC in other ways. Firstly, the affinity of anandamide for CB_1 receptors increases when its non-carboxylic hydrocarbon tail is lengthened and branched. Most notably, as for the alkyl side chain of Δ^9-THC, extension of the non-carboxylic tail of anandamide by two carbon atoms together with the introduction of two methyl substituents, produces an increase in both CB_1 binding affinity and in vivo potency for CB_1 receptor-mediated effects [109, 110]. Secondly, anandamide behaves as an affinity-driven CB_1 receptor agonist. Thus its efficacy at CB_1 receptors, although higher than that of Δ^9-THC, is often found to be lower than that of (+)-WIN55212 or CP55940 (Tables 3, 4 and 6). Thirdly, anandamide has much lower efficacy at CB_2 than CB_1 receptors, lacking detectable CB_2 activity altogether in some experiments (Table 5). These similarities between Δ^9-THC and anandamide are in line with results obtained in molecular modelling studies. Thus Thomas *et al.* [111] have reported that it is possible to superimpose anandamide on the Δ^9-THC molecule such that the oxygen of the arachidonoyl carboxyamide lies over the pyran oxygen, the hydroxyl group of the arachidonoyl ethanol over the phenolic hydroxyl group, the five terminal arachidonoyl carbons over the hydrophobic pentyl side chain and the arachidonoyl polyolefin loop over the tricyclic ring system. A fuller account of the structure-activity relationships in the anandamide series is to be found in two recent papers [45, 108]. It should be noted that the maximal effects of anandamide are not always less than those of WIN55212 or CP55940 (Tables 4 and 6). For example, in AtT-20 cells transfected with rat CB_1 receptors, the inhibition of an inwardly rectifying potassium current by 300 nM anandamide has been found to match the maximal inhibitory effect of WIN55212 [13].

Because anandamide is susceptible to hydrolysis by fatty acid amide hydrolase, in vitro assays of this agent are often carried out in the presence of an enzyme inhibitor such as phenylmethylsulphonyl fluoride [1, 2]. The extent to which anandamide has to be protected from enzymic hydrolysis in this way can be affected by the assay conditions used [1]. In binding assays, for example, there is evidence that whilst there may be a need to protect anandamide from enzymic hydrolysis when a filtration method is used to separate tissue samples from unbound radioligand, this precaution is not needed when the separation is achieved by centrifugation (all [^{3}H]HU-243 experiments in Table 2) [112]. In some cannabinoid receptor-containing tissue preparations, the potency of anandamide is not enhanced by phenylmethylsulphonyl fluoride. This may be because these preparations lack significant fatty acid amide hydrolase activity. However, it could also be because they are unable to take up anandamide from its presumed extracellular site of action, there being evidence that fatty acid amide hydrolase is located intracellularly so that released anandamide is only metabolized after it has been taken up into tissues both by a carrier-mediated process and by passive diffusion [5, 108].

The finding that anandamide is the substrate of an endogenous amide hydrolase has stimulated the development of several analogues that are less susceptible to enzymic hydrolysis. One of these is (R)-

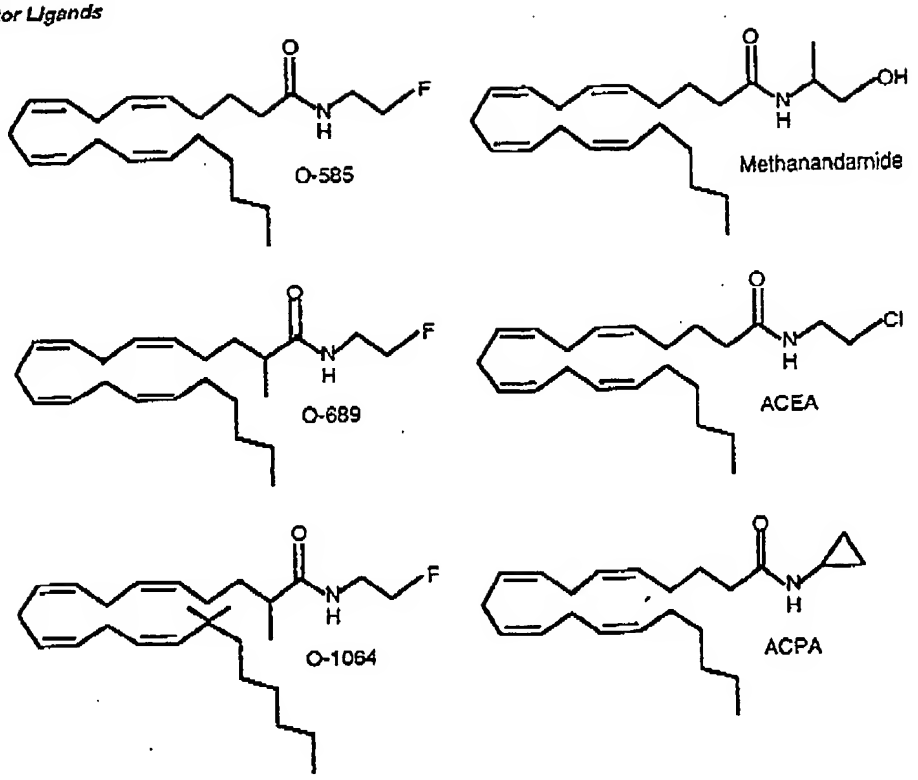

Fig. (11). Structures of some synthetic eicosanoid cannabinoids.

(+)-arachidonoyl-1'-hydroxy-2'propylamide (methanandamide; Fig. **11**) [113]. Unlike anandamide, methanandamide possesses a chiral centre, its (R)-isomer possessing 9-fold higher CB_1 receptor affinity than its (S)-isomer [113]. Another analogue that shows resistance to enzymic hydrolysis is 2-methylarachidonoyl-(2'-fluoroethyl)amide (O-689; Fig. **11**) [114] and it is noteworthy that both O-689 and methanandamide have an enhanced selectivity and affinity for CB_1 receptors (Table 2). Two anandamide analogues with even greater selectivity (and affinity) for CB_1 receptors are arachidonoyl-2'-chloroethylamide (ACEA) and arachidonoylcyclopropylamide (ACPA) (Table 2 and Fig. **11**). The E_{max} values of both analogues, determined in the cyclic AMP assay using CHO cells transfected with human CB_1 receptors and in the GTPγS assay using rat cerebellar membranes, match those of the high-efficacy agonist, CP55940 [46]. However, ACPA (but not ACEA) was found to have a significantly lower E_{max} than CP55940 for inhibition of electrically-evoked contractions of the mouse isolated vas deferens. Neither ACEA nor ACPA showed any sign of reduced susceptibility to enzymic hydrolysis [46].

Two other anandamide analogues of note are N-(4-hydroxyphenyl) arachidonylamide (AM404) and methyl arachidonyl fluorophosphonate (MAFP) (Fig. **12**) [40, 115, 116]. AM404 inhibits anandamide uptake by rat cultured cortical neurones (EC_{50} = 1 μM) and astrocytes (EC_{50} =5 μM) without also producing detectable inhibition of FAAH or inhibiting the uptake of the anandamide metabolites, arachidonic acid and ethanolamine [116]. In line with its properties, AM404 has been shown to potentiate some effects of anandamide, for example anandamide-induced inhibition of forskolin-stimulated cyclic AMP production by rat cultured cortical neurones, anandamide-induced antinociception in the mouse hot plate test and anandamide-induced hypotension in anaesthetized guinea-pigs [116, 117]. AM404 also binds to CB_1 receptors at micromolar concentrations (Table 2). However it does not behave as a direct cannabinoid receptor agonist [116] and its ability to potentiate anandamide suggests that it does not exert any significant degree of cannabinoid receptor antagonism either. MAFP is an irreversible ligand for the CB_1 receptor (EC_{50} = 20 nM for displacement of [^{3}H]CP55940 from specific binding sites on rat brain membranes) and also an irreversible inhibitor of FAAH (EC_{50} = 2.5 nM) [115]. As expected from its binding properties, MAFP (1 μM) has also been shown to produce insurmountable antagonism of several cannabinoid receptor agonists in the myenteric plexus-longitudinal muscle preparation of guinea-pig small intestine, a functional CB_1 receptor assay system [118]. Other fatty acid derivatives that have proved to be potent irreversible inhibitors of FAAH are a series of saturated fatty acid sulphonyl fluorides [119, 120]. The most notable of these is stearyl sulphonyl fluoride

(AM381) as this shows the greatest separation between potency for FAAH inhibition (EC_{50} = 4 nM) and ability to bind to CB_1 receptors (EC_{50} = 18.5 μM for displacement of [^{3}H]CP55940 from specific binding sites on rat forebrain membranes). This is far greater than the 8-fold separation between FAAH inhibitory potency and CB_1 binding potency shown by MAFP. When taken together, the results obtained with stearyl sulphonyl fluoride and AM404 suggest that the structural prerequisites for inhibiting FAAH are not the same as those for inhibiting anandamide uptake or for binding to cannabinoid receptors. There is also evidence that the structural features that determine the ability to inhibit the anandamide transporter differ from those that determine the ability to serve as a substrate for the anandamide transporter [6, 121].

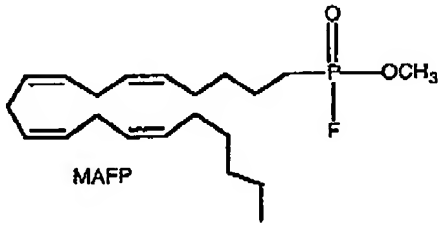

MAFP

palmitoylethanolamide does not have significant affinity for CB_1 receptors in rat brain membranes or in membranes from CB_1 receptor transfected COS cells [112, 123] or show any activity (at 10 μM) as an inhibitor of forskolin-stimulated cyclic AMP production in N18TG2 or rat CB_1 transfected CHO cells [80]. Although the RBL-2H3 cells were found to express CB_2 receptors [122], it is also unlikely that palmitoylethanolamide acted through these receptors. Thus Showalter *et al.* [37] have found that at concentrations of up to 10 μM, palmitoylethanolamide displaces only 20% of [^{3}H](+)-WIN-55212 from binding sites on membranes obtained from human CB_2 receptor transfected CHO cells and that this displacement is not concentration-dependent. Palmitoylethanolamide was found to be even less effective in displacing [^{3}H]CP55940 from these CB_2 binding sites [37]. This finding has been confirmed by Sheskin *et al.* [112] in competitive binding assays using membranes from CB_2 receptor transfected COS cells and [^{3}H]HU-243 as the radiolabelled probe. One possibility is that palmitoylethanolamide is a ligand for a novel type of cannabinoid receptor. Indeed, the suggestion has already been made that palmitoylethanolamide binds to a yet unidentified CB_2

othesis has been
possible explanation

This Page is Inserted by IFW Indexing and Scanning Operations and is not part of the Official Record

BEST AVAILABLE IMAGES

Defective images within this document are accurate representations of the original documents submitted by the applicant.

Defects in the images include but are not limited to the items checked:

- ☐ BLACK BORDERS
- ☒ IMAGE CUT OFF AT TOP, BOTTOM OR SIDES
- ☐ FADED TEXT OR DRAWING
- ☐ BLURRED OR ILLEGIBLE TEXT OR DRAWING
- ☐ SKEWED/SLANTED IMAGES
- ☒ COLOR OR BLACK AND WHITE PHOTOGRAPHS
- ☐ GRAY SCALE DOCUMENTS
- ☒ LINES OR MARKS ON ORIGINAL DOCUMENT
- ☐ REFERENCE(S) OR EXHIBIT(S) SUBMITTED ARE POOR QUALITY
- ☐ OTHER: _____

IMAGES ARE BEST AVAILABLE COPY.
As rescanning these documents will not correct the image problems checked, please do not report these problems to the IFW Image Problem Mailbox.